MSc in Photonics

PHOTONICS**BCN**

Universitat Politècnica de Catalunya (UPC)
Universitat Autònoma de Barcelona (UAB)
Universitat de Barcelona (UB)
Institut de Ciències Fotòniques (ICFO)

http://www.photonicsbcn.eu

Master in Photonics

MASTER THESIS WORK

DESIGN AND TESTING OF A GRADED-INDEX LIQUID CRYSTAL OPTICAL DEFLECTOR

Luis Crespo Fernández

Supervised by Dr. Alejandro Rodríguez Gómez, (UPC-TSC)

Presented on date 20th July 2009

Registered at

Escola Tècnica Superior d'Enginyeria de Telecomunicació de Barcelona

Design and testing of a graded-index liquid crystal optical deflector

Luis Crespo Fernández
Department of Signal Theory and Communications (*TSC*) at Barcelona Tech (UPC)
E-mail: luiscrespo@adtelecom.es

Abstract. A new model of an optical scanning deflector, based on a graded-index deviator, is presented. The deviator is founded on liquid crystal bi-refringence property, permitting the dynamic control of the refractive index of the material through an applied voltage. A simulation tool has been developed to study the deflector behavior and a prototype has been built and tested.

Keywords: liquid crystal, optical deflector, electro-optics, graded-index, simulation.

1. Introduction

Optical deflectors have been used in a wide range of applications, from marking applications [1] to optical links [2].Some of them are based on micro-electromechanical systems, now a growing market [3]. Another group of deflectors is founded on acousto-optic principle [4], in which there is a change of a material's permittivity due to a mechanical wave. Other deviators are based on an optical phased-array [5] or rely on magneto-optic or electro-optic properties of some materials. Usually, deviators without mechanics have a narrow angular range [6].
We present a new electro-optical deflector device [7] based on electro-optical properties of liquid crystal in which a graded-index is induced by the voltage applied in three electrodes. This system permits to scan a wide angular range without mechanical elements.
First we will study the basics of the deflector; later on we will focus on the simulation of the deviator and the properties of the device. Finally, we will show the experimental results through the first deflector prototype.

2. Deflector basics: graded-index in a liquid crystal material

If a beam is propagated through a material with a graded refraction index the wavefront is tilted and the beam is deflected. In the equations we will use the axis z referring to the propagation axis and x as the graded-index axis. Deviation is independent of y axis. Figure 1 describes the trajectory of the incident beam propagated through a linear graded-index medium with dimensions $\Delta x = W$ (width of the cell) and $\Delta z = L$ (depth of the cell). The trajectory could be described through the equations:

$$X(z) = \frac{1}{n}\frac{\partial n}{\partial x}\frac{z^2}{2} = \frac{1}{2}\frac{\Delta n}{n}\frac{z^2}{W} \quad (1)$$

$$\theta_{input}(z) = \frac{1}{n}\frac{\partial n}{\partial x}z = \frac{\Delta n}{n}\frac{z}{W} \quad (2)$$

$$\theta_{output}(z) = \frac{\partial n}{\partial x}z = \Delta n\frac{L}{W} \quad (3)$$

X(z) corresponds to the beam displacement from the *z* axis inside de deviator, being *n* the nominal refractive index and *Δn* the corresponding maximum difference. θ_i y θ_o are respectively the angular values of deviation inside and outside the cell, both linked by the Snell's law in *z=L*.

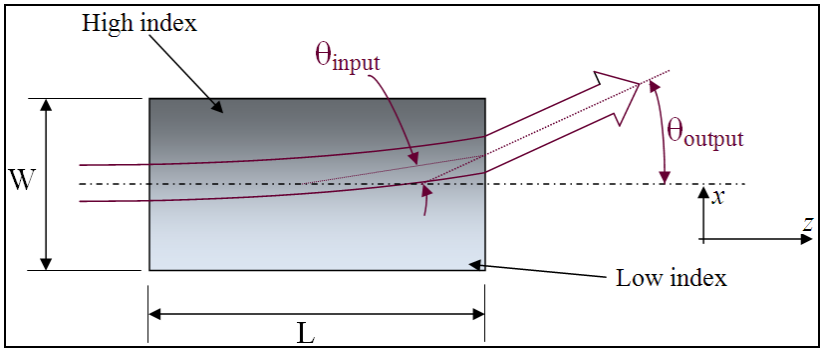

Figure 1 – Basics of an electro-optical scanner [8]

A graded-index profile is produced thanks to the electro-optical properties of liquid crystal. The liquid crystal [9] [10] (abbreviated LC) is a mesophase generated during the crystal and liquid transition of some organic molecules. Most of commercial liquid crystals are thermotropic, i.e. they reach a certain mesophase by temperature variation. Depending on the type of liquid crystal, we have nematic, smectic or chiral liquid crystals. LC molecules are usually elongated (called calamitic or rod-shaped), with a length of about some dozens Angstroms. The main interest of liquid crystal resides on the fact that their molecules act as electrical dipoles: on applying an electric field, liquid crystal molecules tend to be aligned with the electric field, position in which they reach the minimum energy state. Liquid crystal is birefringent, meaning that it possesses two different indices of refraction: one index of refraction corresponds to light polarized along the director of the liquid crystal, and the other is for light polarized perpendicular to the director. The LC refraction index varies from ordinary index (n_o) to extraordinary index (n_e). The molecules tend to be aligned with the electric field faster or slower depending on the intensity of the field and the viscosity degree of the material. When no electric field applied, LC molecules tend to recover their steady-state orientation, which could be forced by rubbing techniques [11].

In our prototype we have used the Merck liquid crystal reference BL087[12], which shows positive anisotropy and uniaxial properties. The refractive index variation value of BL087 is 0.2362, varying from 1.5246 (ordinary index) to 1.7608 (extraordinary index). It shows also short time response, with a viscosity of 47mm^2/s.

The details of the prototype are described in section 3.

3. Optical deflector

3.1. Design of the cell

To reach the linear-graded index described in section 2, the molecules of liquid crystal situated on the left-hand side of the cell must be oriented vertically and sloping down progressively along the *x* axis. The LC molecules situated at the right-hand of the cell are oriented horizontally, as shown in Figure 2.

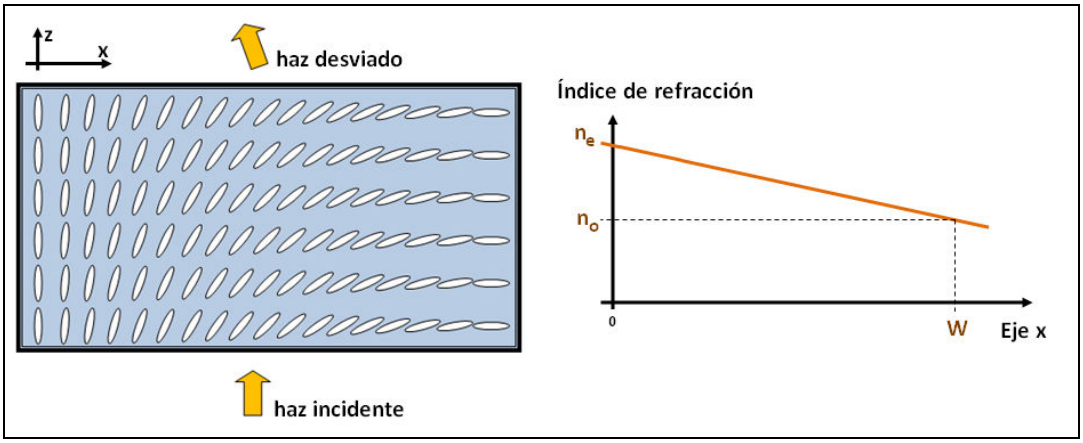

Figure 2 - Progressive inclination of LC molecules.

Among all the possible configurations studied in order to reach a graded-index cell, we will stress on three simple designs, shown in Fig.3:

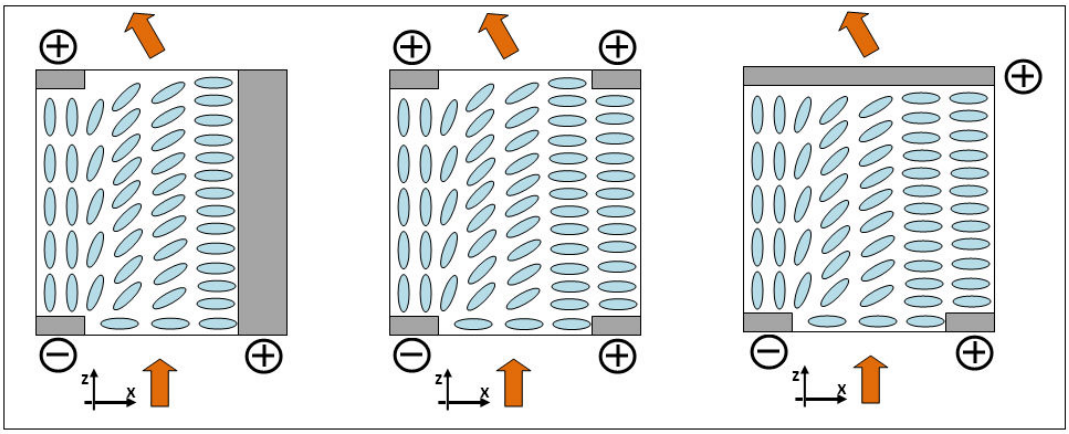

Figure 3 – Main studied designs: a) Vertical electrode. b) 4 electrodes. c) 3 electrodes.

- *Cell with a vertical electrode:* Two electrodes with opposite polarities (left) induce a vertical electric field, whereas a vertical electrode (right) induces horizontal field lines.
- *Cell with 4 electrodes:* In a distribution in which, among 4 electrodes, one of them has an opposite polarity respecting to the others, a vertical electric field is induced on the left-hand side of the deflector, whereas the electric field tends to zero on the right-hand side and thus the molecules preserve their steady-state.
- *Cell with 3 electrodes:* This cell is a simplification of the previous cell, with a unique electrode instead of the two electrodes at the top of the cell.

In order to fabricate a first prototype, the cell with a vertical electrode may be rejected because its configuration is in contradiction with traditional multi-layer deposition techniques. The

second design entails difficulty because of the mechanical alignment necessary to line up higher and lower electrodes, and that could be insurmountable for deep cells. Thus we will focus on the study of the third configuration: the cell with 3 electrodes.
Lower electrodes will be called electrodes 1 and 2 (left and right respectively) and the higher electrode will be called electrode 3. Their associated voltages are V1, V2 and V3.

3.2. **Simulation tool**

A modeling tool has been developed to characterize the deflecting cell and combining the electrostatic calculus of the electric field inside the cell with an optical propagation simulation of a light beam through the previous material.
In the electrostatic calculus, the performing elements are simulated: a glass acting as a substrate, in which are deposited two thin metallic films acting as electrodes and a liquid crystal layer between the substrates. Due to the dielectric anisotropy of the liquid crystal, the electric field of the cell is being calculated iteratively until reaching a convergent value, simulating the electric dipoles of LC molecules.
Once the cell is simulated and the optical system is completely characterized, the propagation through the previous system of a Gaussian beam is simulated through a BPM algorithm, acronym of Beam Propagation Method [13] [14] [15]. It consists of a computational technique which approximates the Helmholtz equation and simplifies the propagation of a certain perturbation in two steps: firstly the Fourier's propagation is simulated in a homogeneous medium and secondly the phase shift induced by the inhomogeneity of the medium is calculated. This two-steps process, represented in Fig.4, will be repeated iteratively along z axis to emulate the propagation of the initial beam through the cell.

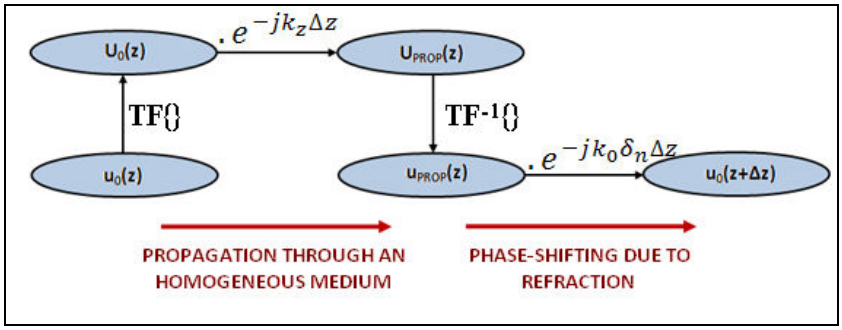

Figure 4 – BPM algorithm scheme.

The BPM algorithm calculus has been compared with theoretical models in the different processes involved in the cell propagation. The simulation of the Gaussian propagation in a homogeneous medium is shown in Figure 5a, Figure **5**b and Figure **5**c represent the diffraction pattern induced by a narrow slot.

According to section 2, if a beam is propagated though a medium with a linear variation of refractive index of slope α, its phase is shifted linearly along the x axis. The deflection introduces then no divergence, even if $\alpha(z)$ varies along the z axis. A Gaussian beam incident to a constantly linear graded-index cell is simulated in Figure 6a, which does not introduces divergence to the beam. In Figure 6b and Figure 6c we simulate the previous cell adding a quadratic variation of factor β which is maximal in the center of the cell. If β is negative, the refraction index curve is concave so the deflected beam diverges when propagated through the

cell (Fig.6b); if β is positive, the curve is convex and the deviated beam converges in a focus deflected from the optical path (Fig.6c)

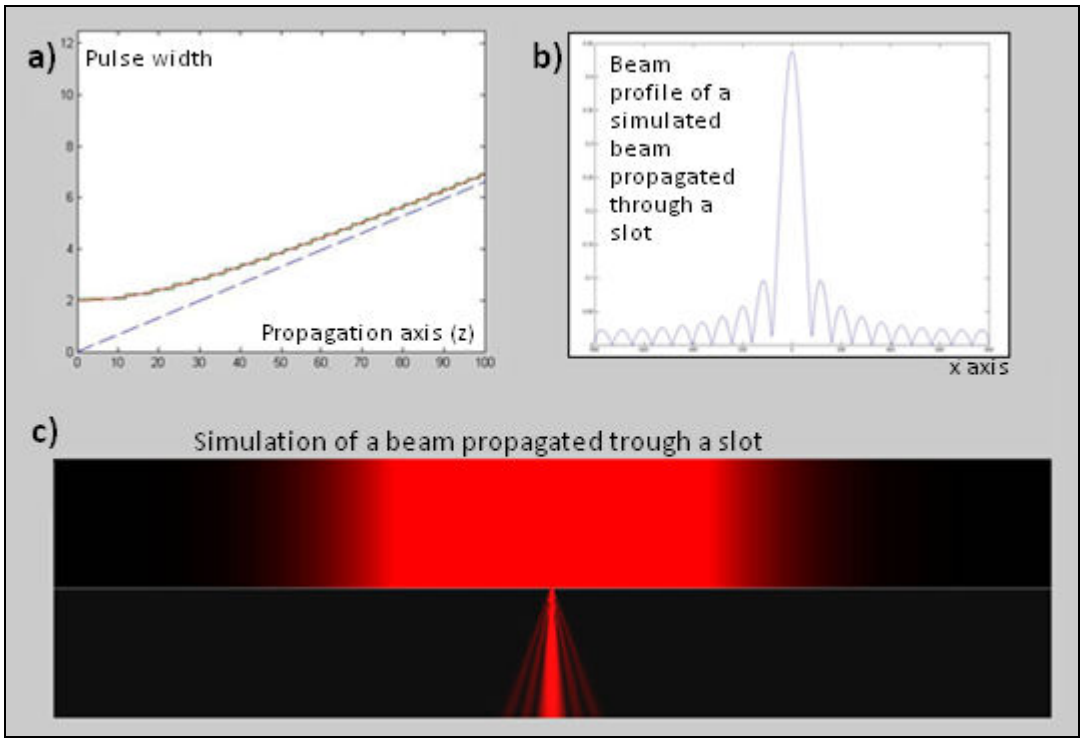

Figure 5 – a) Width of a Gaussian beam propagated through the air. The simulated beam (green) is widened in accordance with diffraction theory (red) and tends to a straight line since the Rayleigh distance. b) c) Simulation of the propagation of a Gaussian beam through a narrow slot (c) and its corresponding pattern (b).

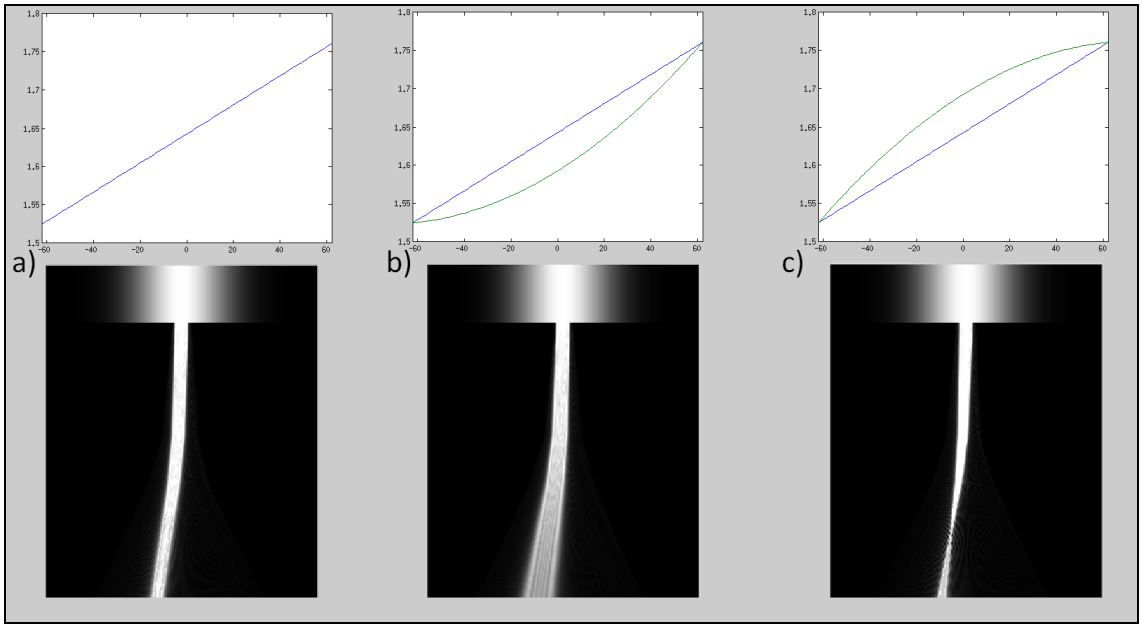

Figure 6 – Simulation of the propagation of a beam through a linear graded-index cell (a) and a variation with a quadratic component (green in b and c) made with the developed tool.

We have also simulated a cell with a β quadratic factor that varies linearly along the z axis from $\beta=-\beta_{max}$ for $z=0$ (as in Figure 6b) to $\beta=\beta_{max}$ for $z=L$ (as in Fig.6c). The phase shifting is compensated along the z axis, so that the cell does not provoke any divergence (as in Figure 6a).

The cell that introduces a linear phase shifting and thus deflects the light without divergence will be considered an ideal cell.

3.3. **Deflecting cell properties**

When the basic distribution of voltages (V1, V2, V3) = (V_0, -V_0, V_0) is applied, the electric field vector goes from electrodes 1 and 3 (positive values of voltage) to electrode 2 (negative voltage). The electric potential associated to that voltage distribution is shown in Fig.7a and the corresponding electric field vector in Fig.7b.

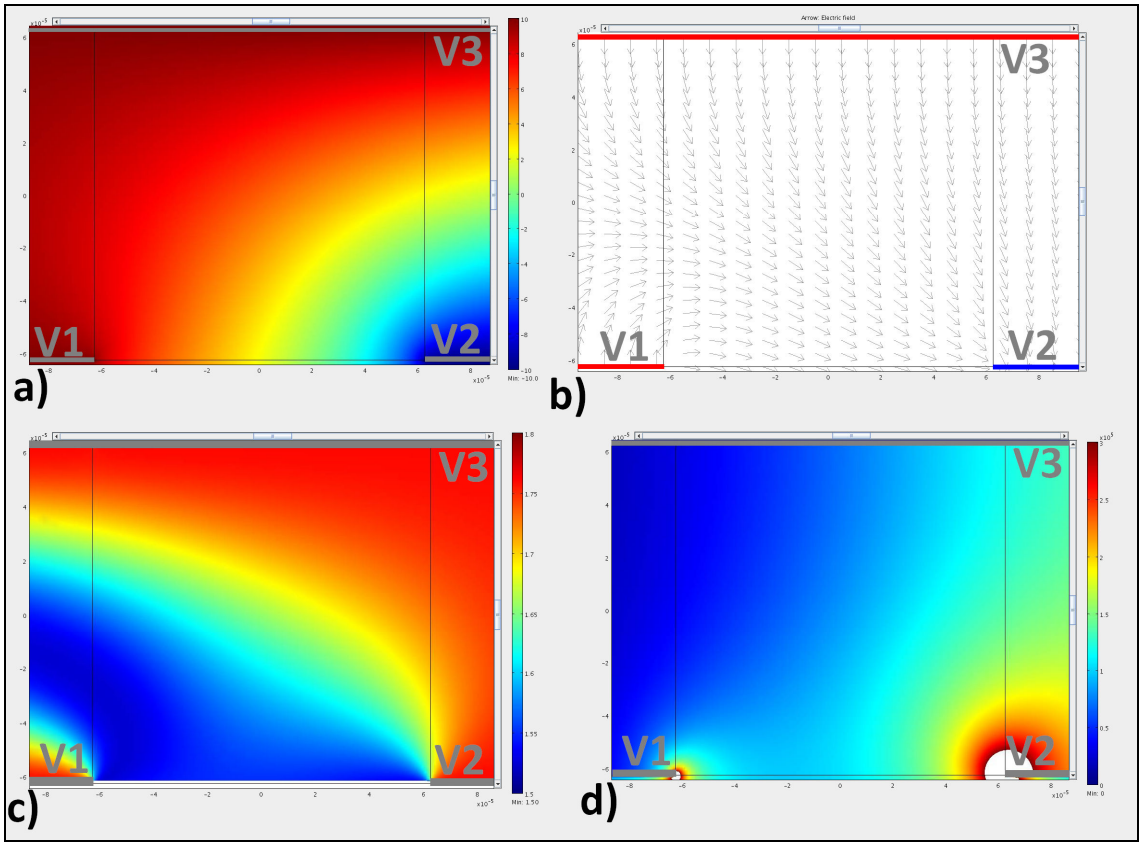

Figure 7 – a) Illustration of the voltage inside the cell when applying a basic voltage distribution (V,-V,V). b) Illustration of the electric field intensity. c) Illustration of the liquid crystal refractive index supposing perfect alignment between LC molecules and the electric field. d) Illustration of the electric field intensity.

According to the uniaxial properties of liquid crystal [5], the refractive index of liquid crystal and the angular inclination of LC molecules θ are linked by the formula:

$$\frac{1}{n_{ref}^{\,2}} = \frac{\cos^2(\theta)}{n_e^{\,2}} + \frac{\sin^2(\theta)}{n_o^{\,2}} \qquad (4)$$

That formula is valid when the electric field intensity is high enough to force LC molecules to be oriented parallel to the electric field lines. In Fig.7c we calculate the refractive index value supposing the field intensity high enough and the molecules perfectly aligned with the electric field lines. No steady-state is then taken into account. However, the modulus values of the electric field given in Fig.7d permit us to estimate molecules inclination according to electric field threshold, the applied voltages and material properties.

The deflector simulation shows the tendency of a graded-index (Fig.7c): the refractive index is in general lower at the left-hand side of the cell than at the right-hand side, but its profile is quite far from the ideal model of deflector exposed in section 3.2. The areas of the cell that do not contribute to the beam deflection will be considered as harmful or useless areas. For instance, in the configuration of three electrodes, the highest area has a constantly vertical electric field vector due to the unique electrode, so the refractive index is constant along the *x* axis and does not contribute to the beam deflection.
On the other side, the intensity of the electric field and the movement speed is reduced if the depth of the cell increases, so that the response time would be lower for deep cells.
The exact graded-index profile and consequent Gaussian beam propagation is defined by the cell dimensions, the applied voltages and the liquid crystal particular properties. Those are parametric input values in the developed simulation tool.

To improve the profile of the graded refractive index in the device, two optimization methods are proposed, taking advantage of the areas with a more linear refractive index variation.
Firstly, we talk about horizontal optimization (or *x* axis optimization) when using a pinhole or slot to demarcate a specific area of incidence of the cell. When reducing the area of incidence, the curve could be better approximated to a linear tangent and the beam is less sensitive to non-linear variations of the refractive index. When reducing the dimensions of the pinhole and consequently the area of incidence, as shown in Fig.8, the divergence introduced by the deflector is decreased. However, if reducing the pinhole diameter excessively, the beam diverges and secondary lobes appear in the beam profile due to diffraction effect.
The developed simulation tool takes also into account the size and shape of the slot, as well as the relative alignment between the pinhole and the center of the cell, which defines the area of incidence.

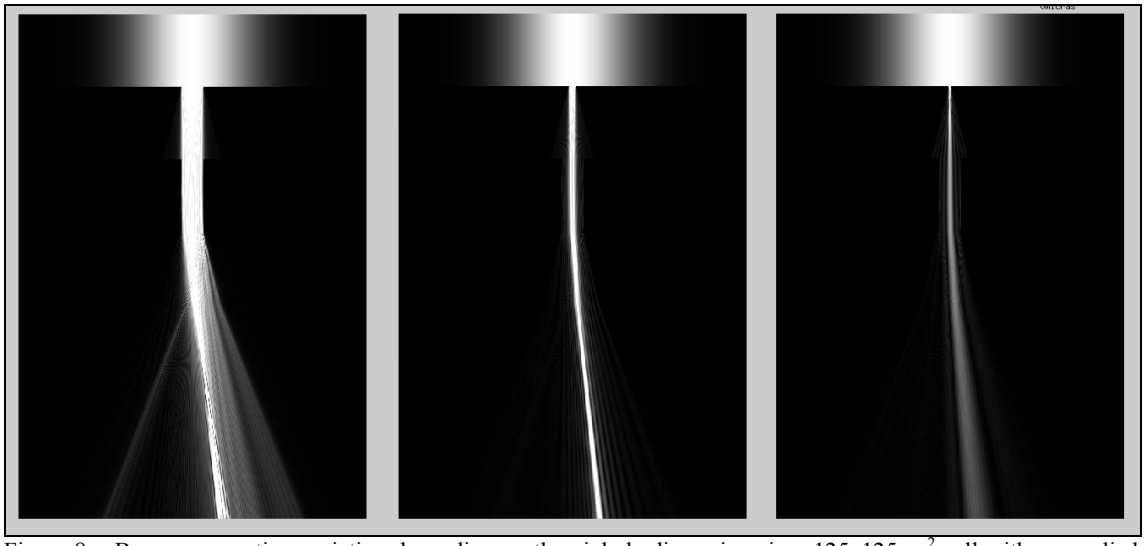

Figure 8 – Beam propagation variation depending on the pinhole dimensions in a 125x125um^2 cell with an applied voltage distribution of (V, -V, V). The simulated pinhole diameters correspond to 125um, 40um and 10um.

On the other hand, we will call vertical optimization (or z axis optimization) referring to the possible use of a dielectric material (without dielectric anisotropy and a constant refractive index) located in the areas of the cell considered as harmful or useless. The liquid crystal will be then confined just in the most linear areas of the cell, and consequently the output beam quality will be improved. Moreover, the effective depth of the cell being reduced, the response time of the cell is also reduced. We will consider possible dielectric layers just on the higher and lower areas of the cell, as if the dielectric materials were deposited on the electrodes, otherwise that would be unfeasible with traditional manufacturing techniques. The simulation tool has been developed taking into account the possible dielectric layer depth and its relative dielectric constant as input parameters to characterize the optical deflector.

3.4. **Scanning mode**

The scanning mode consists of a deviation of the incident beam with an angle varying progressively from $-\theta_{max}$ to θ_{max} in an interval T. The refractive index variation of liquid crystal must be defined as to shift the incident wave phase proportionally to the desired deflected angle. Each voltage distribution induces different electric field lines and a characteristic deflection profile of the beam. The simulation is carried out for a wide range of voltage distributions; subsequently the program extracts those voltage distributions that permit to deflect the beam with a certain angle and with a divergence lower than a defined threshold.
A succession of values that permit to scan the light in a certain angular range could be then defined for each cell configuration. As a matter of fact, just half of the values are required, so a symmetric refractive index variation is reached when inverting V1 and V2 values, because the deflector deviates with an opposite angle. That reduces the computational cost of the calculation.

In Figure 9 we show a scanning deflection system guided by the variation of the applied voltage distributions. Using a pinhole largely narrower than the distance between electrodes 1 and 2 makes easier a guided scanning deflection: the beam is less sensitive to the non-linearity of the refractive index profile of the cell, which are different for each voltage distribution. The pinhole may be located on the plane $x=0$ to reach a symmetric deflection. A scanning deflection of +/- 10º is shown in Figure 9 for a 125x125um^2 cell using a pinhole of 40um.

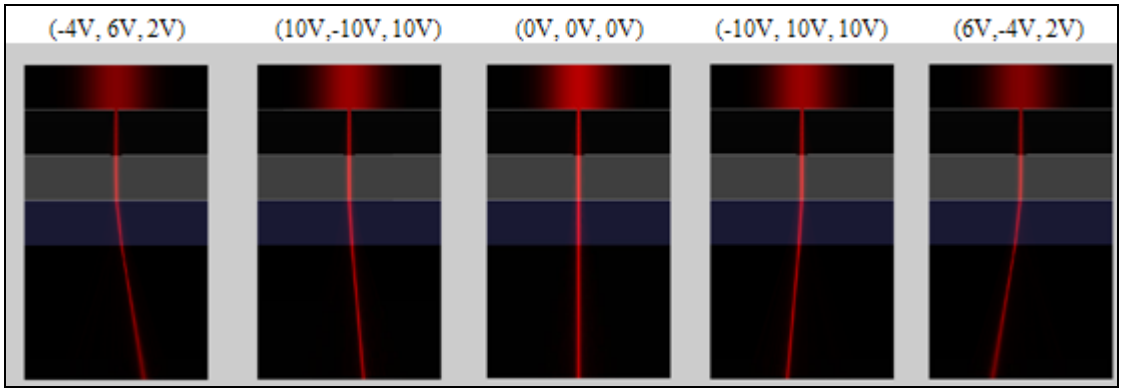

Figure 9 – Beam scanning due to the variation of the applied voltage values.

4. **Fabrication of a prototype**

4.1. **Fabrication process**

In order to validate the basic principles described previously, an optical deflector prototype has been fabricated in collaboration with The Institute of Photonic Sciences (ICFO) [16]. The processes carried out to fabricate the cell include the deposition of a reflective chromium layer onto the glass substrates using a sputtering system and a photolithographic technique to design the electrodes. Every cell is designed as having a width of 125microns, which is the separation of the electrodes in x axis. The mask is designed with strip-shaped electrodes, so that the deflection is independent of y axis. The cell is assembled and sealed using two different optical fibers having a 125um and a 40um diameter respectively. Thus we will distinguish two different cells: cell A (125x125um^2) and cell B (125x40um^2).

4.2. Experimental setup

The experimental setup includes a circularly polarized laser (633nm), a polarizer, a lens with 5cm focal distance focused on the deflector substrate and the deflector. Due to the uniaxial properties of liquid crystal, the system is sensitive to the polarization of the beam: one direction of polarization is propagated without perceiving any anisotropy, whereas the perpendicular polarization perceives the graded-index variation and is in consequence deflected. However, using a lens to demarcate the area of incidence in the cell is useful to study the different parts of the cell, but reduces the experimental repeatability of the experiment. In further designs, a pinhole will be used and integrated to the optical system instead of a lens, as it has been made throughout the simulations.

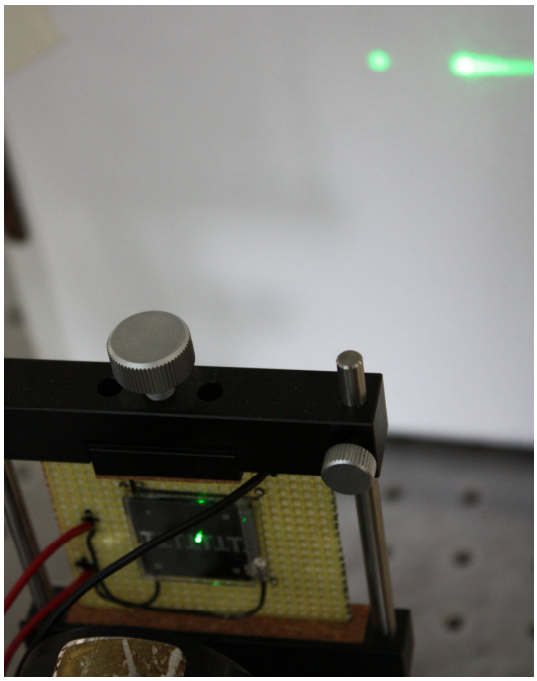

Figure 10 – Optical deflector prototype photography

Once proved the deflecting principle, the following hypotheses have been experimentally confirmed:

- Due to the low ratio L/W, the 125x40um^2 cell introduces a minor phase shifting than the 125x125um^2. The deflection angle when propagating through cell A is thus higher than the angle provoked by cell B.
- Due to its reduced depth, the response time of cell B is lower than the response time of the square cell A. Reducing the parameter L, the intensity of the electric field increases and the LC molecules can move more easily, which reduces the time response.
- The scanning principle proposed in 3.4 is verified applying the voltage distributions previously simulated. The angle of deflection depends on the applied voltages and thus the device acts as an optical scanner.

5. Conclusions

This article describes a new type of optical deflector: we have presented its design, simulated the cell, and studied its principal properties. A first prototype has also been fabricated and tested in order to validate the conclusions of the simulations. We have developed a simulation tool

which integrates the electrostatic and optical calculus of the system to characterize the cell and a beam that is propagated through the cell. The input parameters are the dimensions of the cell, the electrooptical properties of the liquid crystal and the characteristics of a possible pinhole or dielectric layer. The deflecting principle has been proved experimentally and the deflector acts as an optical scanner in a range of +/-10º. We have also demonstrated that the response time is lower in a 125x40um^2 than in a 125x125um^2 cell, and that it has a lower deflection angle.

Acknowledgments

I would like to express my gratitude to Alejandro Rodríguez, Federico Dios and Adolfo Comerón for their suggestions and discussions, to Pedro Martínez, Xavier Martínez, Antonio Alcayde and all the staff of ADTelecom, S.L. for its collaboration in the project. I would like to acknowledge Luis Martínez and Valerio Pruneri for their experimental contribution. I would like to make special mention to Cristina, my friends, my parents and my family for their unconditional support.

References

[1]Ravellat, Ramon S, 1991, *System for marking moving objects by laser beams*, Castellar Del Valles, United States Patent 5021631

[2] Michael A Grant, David Robson , 1990, *Optical communications apparatus for sending optical transmissions to a plurality of remote stations,* United States, Patent 4933928

[3] Manouchehr E. Motamedi, 2005, *MOEMS: Micro-Opto-Electro-Mechanical Systems*, SPIE Press, Bellinham, Washington, USA.

[4] Bahaa E. A. Saleh, Malvin Carl Teich, 1991, *Fundamentals of Photonics*, John Wiley & Sons, Inc., chapter 20, p.799-831

[5] Jay Stockley and Steve Serati, 2004, *Beam combining using a Phased Array of Phased Array,* Boulder Nonlinear Systems, Inc., 450 Courtney Way, Lafayette, CO USA 80026

[6] Jay Stockley and Steve Serati, *Advances in liquid crystal beam steering*, Boulder Nonlinear Systems, Inc., 450 Courtney Way, Lafayette, CO USA 80026

[7] Daniel D. Stancil, 2003, *Electro-Optical Scanners* (New York: Marcel Dekker)

[8] Jean-Pierre Huignard, Jean-Paul Pocholle, 2003, *Electro-Optical Materials* (New York: Marcel Dekker)

[9] B Bahadur, 1992, *Liquid crystals - Applications and Uses,* Litton Systems Canada, Toronto, Canada

[10] Sven T. Lagerwall, Per G. Rudquist, David S. Hermann, 2003, *Liquid Crystals—Optical Properties and Basic Devices* (New York: Marcel Dekker)

[11] Fu-Lung Chen, Ted-Horng Shinn, Chein-Dhau Lee , Wen-Shiang Wang, 1999, *Design, synthesis and properties of polyimide alignment materials,* Materials Research Laboratories, (Taiwan)

[12] http://www.merck.de/company.merck.de/en/images/Aktiv-Matrix_engl_tcm82_16325.pdf

[13] Robert R. McLeod, *Fourier beam propagation*, ECE 6006 Numerical Methods in Photonics, University of Colorado

[14] Federico Dios, Jaume Recolons, Alejandro Rodríguez and Oscar Batet, 2008, *Temporal analysis of laser beam propagation in the atmosphere using computer-generated long phase screens* Universitat Politècnica de Catalunya. Vol. 16, No. 3 / OPTICS EXPRESS

[15] Federico Dios, Juan Antonio Rubio, Alejandro Rodríguez, and Adolfo Comerón, 2004, *Scintillation and beam-wander analysis in an opticalground station–satellite uplink***,** APPLIED OPTICS _ Vol. 43, No. 19

[16] Luis Martínez, Valerio Pruneri, 2009, *Design, fabrication and characterization of a liquid crystal-based light deflector,* ICFO (Castelldefels)